2-2023

Tree stem volume estimation from terrestrial lidar point cloud by unwrapping

Zhongming An
Michigan Technological University, zan1@mtu.edu

Robert E. Froese
University of Alberta

Canadian Journal of Forest Research

OPEN ACCESS | Article

Tree stem volume estimation from terrestrial LiDAR point cloud by unwrapping

Zhongming An[a] **and Robert E. Froese**[b]

[a]College of Forest Resources and Environmental Science, Michigan Technological University, 1400 Townsend Drive, Houghton, MI 49931 USA; [b]School of Forest Science and Management, University of Alberta, 751 General Services Building, Edmonton, AB T6G 2H1, Canada

Corresponding author: **Zhongming An** (email: zan1@mtu.edu)

Abstract

Estimating the volume of standing trees is a fundamental concern in forestry and is typically accomplished using one or more measurements of stem diameter along with formulae that assume geometric primitives. In contrast, technologies such as terrestrial Light Detection And Ranging (LiDAR) can record very detailed spatial information on the actual surface of an object, such as a tree bole. We present a method using LiDAR that provides accurate volume estimates of tree stems, as well as 2D rasters that display details of stem surfaces, which we call the "unwrapping method." This method combines the concepts of cylinder fitting, voxelization, and digital elevation models. The method is illustrated and tested using a sample of standing trees, whereby we are able to generate accurate volume estimates from the point cloud, as well as accurate visualization of the scanned stem sections. When compared to volume estimates derived from Huber's, Smalian's, and Newton's formulae, the differences are consistent with previous studies comparing formula-derived volume estimates and water-displacement-derived volume estimates, suggesting the unwrapping method has comparable accuracy to water displacement.

Key words: volume estimation, stem volume, LiDAR, QSM, voxelization

Introduction

A forest can provide many resources such as wood, fiber, and food, and ecosystem services like water supply and environment mitigation, but for landowners, financial return is one of the common goals, and the volume of the tree stem is one of the major contributing factors to those financial goals. Traditionally, the volume of stem segments, commonly called logs, may be derived from diameter measurements of downed trees using formulae associated with geometric forms, such as Huber's, Smalian's, and Newton's formulae (Avery and Burkhart 2002). The accuracy of these formulae obviously depend on how accurately the underlying geometric form represents the actual form of a log. A very accurate way of measuring volume is to use a water displacement method, where the downed and segmented tree will be submerged under water and the volume of the displaced water will be the volume of the segmented tree (Martin 1984; Biging 1988; Filho et al. 2000). However, both methods usually involve cutting down trees, which could only be performed on trees that are to be harvested and measuring volume by submersion is obviously impractical in virtually any operational setting. Taking measurements at various heights along the bole of a standing tree can be done with devices such as a Tele-Relaskop (Parker 1997) to estimate those diameters, but it cannot be as accurate as a direct measurement, especially with irregular shaped stems. Direct measurements can be taken from the upper stem as well, but will require climbing equipment and training of the operator, which introduces more risk during data collection, and is more time consuming. Thus, it is possible but impractical to perform such missions in real life. With terrestrial laser/LiDAR scanning (TLS), on the other hand, a very detailed point cloud of a stem could be obtained and an accurate volume estimate could be obtained from the detailed point cloud, which could be very useful especially on standing trees.

Methods for obtaining log volume estimates from LiDAR point clouds is an area of active contemporary research. A common approach is fitting primary geometries, such as cylinders, to a LiDAR point cloud capturing the tree stem (Thies et al. 2004; Hackenberg et al. 2015; Olschofsky et al. 2016). Cylinder fitting often requires the tree point cloud being separated into many short stem segments, and thus algorithms for such action also developed. Quantitative structural modeling (QSM) (Raumonen et al. 2011; Åkerblom et al. 2012; Raumonen et al. 2013) is a method combining tree segmentation and cylinder fitting. QSM has been a popular method used for studies such as radiative transfer modeling (Calders et al. 2018) and non-destructive biomass/volume modeling (Calders et al. 2014; Hackenberg et al. 2015; Sun et al. 2016; Stovall et al. 2018). Other than cylinders, additional basic shapes can also be used; for example, Åkerblom

et al. (2015) suggested that cylinders be used for branch reconstruction and, if necessary, more complex shapes can be used for stem reconstruction. Voxelization of the point cloud is another way of estimating tree volume from a LiDAR point cloud, whereby the total volume of the voxels is the estimated volume of the tree, which could be more accurate than the traditional method depending on the size of the voxels (Moskal and Zheng 2012;Hauglin et al. 2013; Hosoi et al. 2013; Bienert et al. 2014). Cylinder fitting may provide an adequate estimate of the volume of a log, but the details of the surface is often lost during the process. In contrast, voxelization provides an accurate estimate of volume as well as a good amount of detail from the LiDAR point cloud, but this depends on the size of the voxel, and the process requires some sort of filling procedure (Moskal and Zheng 2012; Hauglin et al. 2013; Hosoi et al. 2013; Bienert et al. 2014) since the LiDAR points only cover the surface.

LiDAR is also often used to generate digital elevation models (DEMs) of the earth's surface (Ma 2005; Shan and Sampath 2005; Liu 2008), which can be considered as pixel-based raster, with each pixel storing the elevation value. DEMs can be used to calculate volumes and observe changes in volumes (McNabb et al. 2019; Grohmann et al. 2020); we propose that the same concept can be applied to tree stems. Instead of using an ellipsoid or a geoid for elevation of the earth surface, cylinders can be used as the primal geometry for tree stem surface. In this model, a height map like a DEM can be generated and thus the volume of the stem can be estimated. In this study, we combine the concept of cylinder fitting and voxel-base volume estimation, as well as volume estimation from DEMs, and propose an alternative stem volume estimation method, which we call the "unwrapping" method. This method is similar to freeform curve fitting method to obtain stem diameters and cross-sectional profiles (Gollob et al. 2020; You et al. 2021), where Cartesian coordinates of a slice of stem point cloud are converted to polar coordinates and subsequently a curve, such as a spline, is fitted to the converted points. This method better preserves the general profile and possibly much more detail from a TLS point cloud, as well as stores the information of a processed stem in a simpler form, as a two-dimensional (2D) raster. Also, if properly visualized, the information could aid in estimating standing tree grade through the capture of major stem blemishes, such as branches, cracks, and other bole defects in the TLS scan. For example, Stängle et al. (2014) showed that TLS not only could capture surface defects, but measurements of those defects could predict inner wood quality attributes such as knotty core and maximum knot size as measured using X-ray computed tomography (CT).

The overall goal of this study is to present and demonstrate the unwrapping method. We describe test data obtained from a number of standing trees, measured both manually (using diameter tapes) and scanned to generate point clouds. We describe the geometry of the unwrapping method, and the workflow used to calculate log volumes from the point cloud. We expect that volume differences between the unwrapping method, which is derived from TLS point clouds, and conventional volume equations, which use diameter measurements and assume particular geometry, are similar to the differences between water displacement method and volume equations.

Materials and methods

Approach

The unwrapping method was developed and applied to a test sample of mature trees, of three species typical of the northern hardwood region. Species were red pine (*Pinus resinosa* Ait.), sugar maple (*Acer saccharum* Marsh.), and quaking aspen (*Populus tremuloides* Michx.). Each test tree was both scanned to generate point cloud data and then manually measured (standing live, using ladders and a diameter tape) to generate reference data for modeled volume comparisons.

Point cloud data collection

Sampled trees were selected on the campus of Michigan Technological University, located in Houghton, MI, USA. LiDAR scanning was performed in May 2021, using a FARO X330 phase shift scanner. The selected trees are sparsely located with little ground vegetation and thus the scans were able to capture most of the lower tree boles without obstruction. In total, five sphere targets with radii of 7 cm were available and, during the data collection, stations were set up such that at least four spheres were visible for each station, and each station could cover a 90° angle to speed up data collection. Scans were later registered in CloudCompare (version 2.12, 2021).

Reference measurement

Field measurements were obtained in June and July of 2021. Trees were measured live and standing, and thus climbing gear, ropes, and a tree ladder were deployed so that direct measurements could be made using a diameter tape. Diameters were measured at 0.61 m (2 ft) intervals from the ground level to 4.88 m (16 ft) above ground, and in total, 81 measurements were taken for the nine trees. An exception was made for one aspen, which was measured from 0.61 m (2 ft) to 5.49 m (18 ft) to obtain a 4.88 m (16 ft) log section, since ground vegetation was not completely cleared and caused significant occlusion at ground level. Also, one of the maples has an irregularity in the bole (a large bump) at about 2.4 m (8 ft) in height, and thus the diameter measurement above the bump, which is at about 2.6 m (8.4 ft) in height, was used instead.

Tree point cloud processing

Standing tree scans were first registered manually in CloudCompare using sphere targets set up during data collection to obtain a full 3D point cloud for each stem. Once all scans were correctly registered, clip boxes were applied to each registered point cloud to remove excessive surroundings. A Cloth Simulation Filter (CSF, Zhang et al. 2016) was applied to the point cloud to separate ground and non-ground points, and subsequent processes were performed on the non-ground points. Preliminary foliage and other noise point reduction was accomplished by using a simplified method inspired by Zhang et al. (2019), which uses curvature change

Fig. 1. A cylindrical coordinate system.

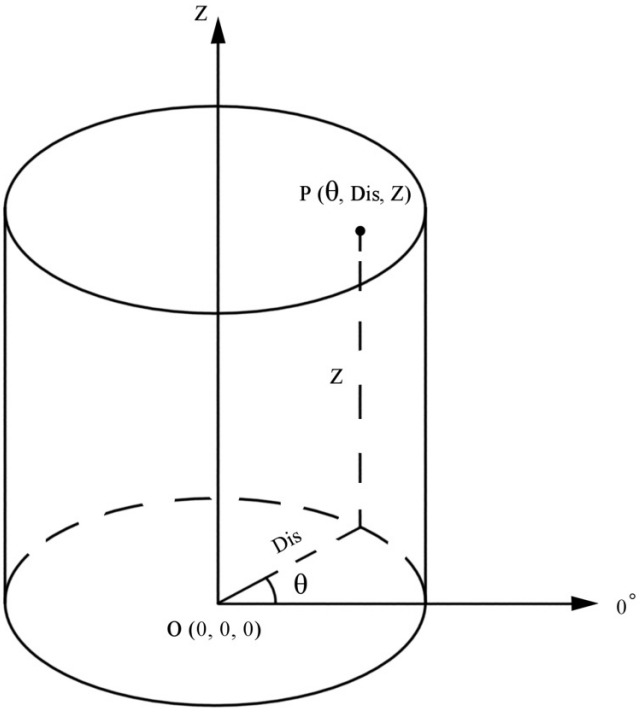

Fig. 2. How roll, pitch, and yaw are defined in this study.

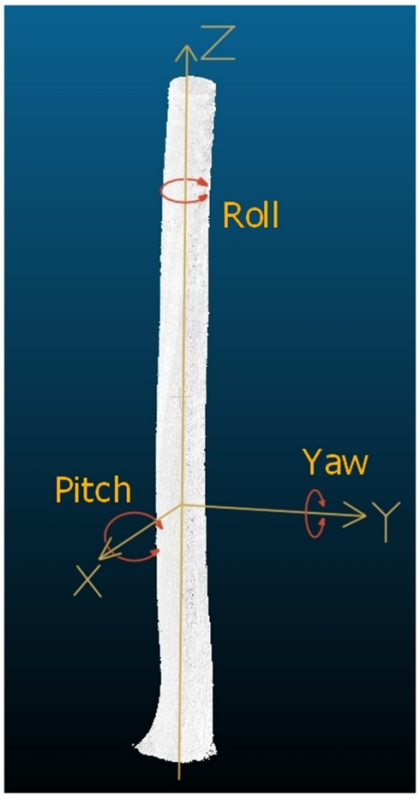

rate to filter out many of those points. In this case, geometric features were calculated within CloudCompare, and PCA2, the second eigenvector of principal component analysis (PCA), was used as the parameter to set the threshold, which is less likely to filter out stem points and leave holes in the stem. The thresholds used in this case vary from 0.2 to 0.4, depending on the visual inspection. After filtering, connected components were labeled to separate clusters of points, and the stem points were selected from the clusters and exported as individual point clouds for later manual cleaning. Once individual stems were separated, and branches and remaining foliage and noise points manually removed, a section of the lower tree bole 4.88 m (16 ft) in length was then selected and exported for further processing.

Coordinate transformation

For a mostly straight tree stem, an axis should go through the stem and around the axis, the surface of a stem can be unwrapped into a 2D plane, and thus generate a model like a DEM. The point clouds collected by the LiDAR unit were in local Cartesian coordinate systems defined by the scanner, and by converting points to cylindrical coordinates (Fig. 1), the point cloud can be unwrapped. The first step is to find the central axis, achieved by performing PCA on the stem sections, where the first eigenvector and the center point decide the central axis. Then a coordinate transformation between Cartesian coordinate systems moves the center of the stem to (0, 0, 0) and converts the first eigenvector to (0, 0, 1), and thus the central axis is the *Z* axis of the converted coordinate system. In this case, the rotation matrix was generated using the roll, pitch, and yaw fashion, where, for the stem section, the rotation along the central axis was considered as roll, the rotation along the *X* axis was considered as pitch, and the rotation along the *Y* axis considered as yaw (Fig. 2). The rolls for the stem sections were all set to 0 for a simpler transformation process and it does not matter much in this case. Thus, the rotation matrix is

$$(1)\quad R_r = \begin{bmatrix} \cos(r) & -\sin(r) & 0 \\ \sin(r) & \cos(r) & 0 \\ 0 & 0 & 1 \end{bmatrix}$$

$$R_p = \begin{bmatrix} 1 & 0 & 0 \\ 0 & \cos(p) & -\sin(p) \\ 0 & \sin(p) & \cos(p) \end{bmatrix}$$

$$R_y = \begin{bmatrix} \cos(y) & 0 & -\sin(y) \\ 0 & 1 & 0 \\ \sin(y) & 0 & \cos(y) \end{bmatrix}$$

where *r*, *p*, and *y* represent roll, pitch, and yaw, respectively, and *R* represents the rotation matrix.

With the point cloud in the new Cartesian coordinate system, the points were then converted into a polar coordinate system in the XY plane while retaining the *Z* coordinates (Fig. 1), which is a cylindrical coordinate system. Thus, each point was represented as (θ, Dis, *Z*), where θ is the azimuth, Dis is the distance from the point to the central axis, and *Z* is the retained *Z* coordinate from the Cartesian coordinate system. Then let θ

be U; let Z be V; let Dis be W. These variables will then be presented in a Cartesian coordinate system (U, V, W). However, U is represented in angle and to convert angles to a distance, a base cylinder was used where the radius was the absolute mean of the distances and the height is the same as the range of Z, of which the circumference represents a 2π range. Thus, the U coordinates were consistent with V and W and then the coordinates were exported for later processing in ArcGIS.

Interpolated surface generation

Surface rasters were generated from the point coordinate layers using the inverse distance weighting (IDW) in ArcGIS 10.5, with concave hulls to reduce extrapolation. Then rasters with a constant value of 0 and the same size as the respective IDW rasters were created and merged with the IDW rasters, filling the extrapolation pixels with a value of 0. Rasters were then converted to point features with a resolution of 5 mm and exported for subsequent processing.

Volume estimation

Two volume estimation methods were tested. The first defines each pixel as representing a small wedge, of which the volume could be calculated easily; this is referred to as "NC" in the following text. The second uses the volume of the base cylinder as a base volume estimate and each pixel represents the volume difference between the interpolated surface and the cylinder; it will be referred to as "CY." The difference between NC and CY is that NC uses the sum of volumes of those wedges to obtain volume while CY uses a base cylinder volume and adds or subtracts the volume difference between stem surface and the cylinder to obtain volume.

The angle resolution, which is defined as the angle covered by each pixel, was calculated. In the case of the first method, NC, the volume of each pixel wedge was calculated by

$$V_{\mathrm{NC}} = \mathrm{Dis}^2 \times \tan\frac{\varphi}{2} \times \mathrm{Res} \tag{2}$$

where V_{NC} represents the volume of each wedge, Dis represents the distance from the interpolated surface to the central axis, φ represents the angle resolution, and Res represents the pixel size or spatial resolution. The sum of all the pixel wedges is the final estimate of the stem section volume.

In the case of the second method, CY, the volume difference of each pixel was calculated by

$$V_{\mathrm{Diff}} = \frac{\left(\mathrm{Res} + 2 \times \mathrm{Dis} \times \tan\frac{\varphi}{2}\right) \times \mathrm{Diff} \times \mathrm{Res}}{2} \tag{3}$$

where $\mathrm{Diff} = \mathrm{Dis} - R_c$, R_c being the radius of the base cylinder. The sum of the base volume and the volume difference is the final estimate of the stem section volume, V_{CY}.

Traditional volume estimation and data analysis

Volume estimates from TLS were compared to the volume estimates using popular log volume estimation formulae, specifically Huber's, Smalian's, and Newton's formulae (Avery and Burkhart 2002). Huber's formula uses the diameter measurement from the midpoint of a log segment, while Smalian's uses the diameter measurement at the two ends of a segment, and Newton's uses all three diameters. In this study, measurements were taken every 0.61 m (2 ft) to 4.88 m (16 ft) in height; thus, volume was calculated for each of the eight segments using Smalian's formula, and the four segments using Huber's and Newton's formula, and the estimate for the entire log was the sum of the volume of the individual segments.

To be consistent with previous studies, the estimated volumes from TLS were considered as the "true value" and compared to the estimated stem volumes from manual measurements according to different volume formulae. Thus, the difference between "true" and "estimated" volumes were calculated with the following equation:

$$e_i = \frac{\sum_{i=1}^{n}(y_i - \widehat{y}_i)}{n} \tag{4}$$

where e_i is the difference, y_i is the volume estimated by unwrapping, and $\widehat{y}_i$ is volume estimated by formula from diameter measurements.

Results

Measured using a circumference tape, standing tree diameters at the base ranged from about 35 to 85 cm (Fig. 3). The largest trees were the three maples, and the smallest the three pines, with aspen falling in-between. Some trees exhibited marked taper; for example, the diameter of maple Tree 3 declined from over 80 cm at the base to just over 50 cm at about 1.3 m (4.3 ft) in height. Taper was greatest in the largest trees, regardless of species. Note that because a measurement at the base of aspen Tree 3 was not possible, taper at the base is not known for this tree. Note also that the "bump" at about 2.4 m (8 ft) in height for maple Tree 1 is not apparent in the diameter profile from measurements, because the measurement was taken above the "bump" instead.

LiDAR data collection produced a dense point cloud comprised of stem, foliage, and ground returns (Fig. 4). Visual assessment of points removed using foliage and noise filtering reveal that some points that appear to be true stem returns were falsely eliminated. However, these removals did not leave significantly large holes along the stem. Other remaining foliage points were easily removed manually.

Unwrapped LiDAR volume estimates NC and CY were nearly indistinguishable (Table 1; Fig. 3). Volume estimates from stem circumference measurements were always larger than those from LiDAR, with the largest values from Smalian's formula and the smallest from Huber's formula. The absolute mean bias if NC estimates are considered as "true" values is 9.71%, and the absolute mean bias for CY is 10.00%; when compared to volume estimates using Huber's formula, the absolute mean biases for NC and CY are 5.51% and 5.79%, respectively; when compared to volume estimates using Newton's formula, the absolute mean biases for NC and CY are 8.31% and 8.59%, respectively.

Table 1. Summary of volume estimates for the test sample trees, by method.

	Maple 1	Maple 2	Maple 3	Pine 1	Pine 2	Pine 3	Aspen 1	Aspen 2	Aspen 3
NC Vol Est (m^3)	0.603	0.461	0.931	0.330	0.438	0.315	0.563	0.450	0.343
CY Vol Est (m^3)	0.602	0.460	0.930	0.329	0.435	0.313	0.565	0.451	0.340
Smalian Vol Est (m^3)	0.694	0.513	1.147	0.348	0.467	0.326	0.617	0.493	0.354
Huber Vol Est (m^3)	0.652	0.501	1.078	0.342	0.460	0.316	0.571	0.465	0.352
Newton Vol Est (m^3)	0.679	0.509	1.124	0.347	0.464	0.323	0.601	0.483	0.354
NC-Smalian Bias%	14.86	11.13	23.15	5.73	6.41	3.79	9.52	9.27	3.54
CY-Smalian Bias%	15.17	11.33	23.33	6.18	7.04	4.44	9.11	9.05	4.31
NC-Huber Bias%	8.11	8.69	15.82	3.92	5.00	0.53	1.51	3.27	2.74
CY-Huber Bias%	8.40	8.90	15.99	4.36	5.62	1.16	1.13	3.07	3.51
NC-Newton Bias%	12.61	10.32	20.70	5.12	5.94	−2.70	6.85	7.27	3.27
CY-Newton Bias%	12.91	10.52	20.88	5.58	6.57	−3.34	6.45	7.06	4.04

Fig. 3. Tree diameter profile with height (left) and estimates of log volume by method (right).

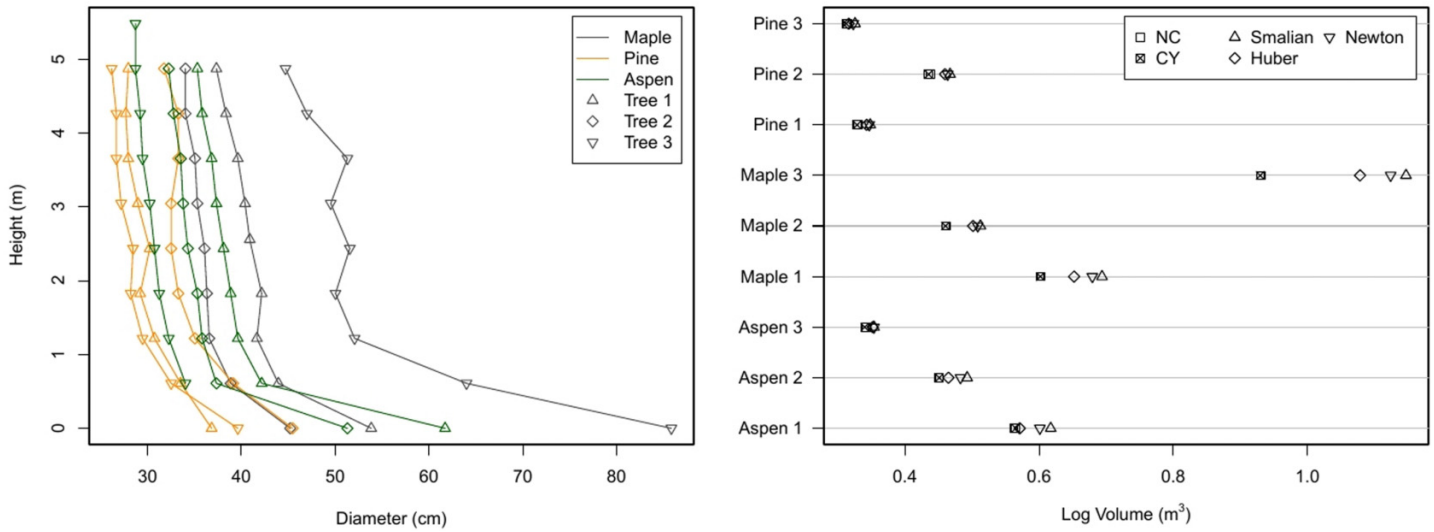

Discussion

In this study, we present a novel method of estimating tree stem volume from a LiDAR point cloud, which effectively "unwraps" a log such that it is represented digitally as a surface model. This method can work not only with TLS data, but point clouds generated from photogrammetry as well, and has some distinctive advantages over alternative approaches. A detailed tree displacement raster can be generated, easily visualized, and is detailed enough to capture some large defects from the stem, such as the large bump of Maple 1 and the scarring tissue above it (Fig. 5). Visualization could be helpful in standing tree grading, through detection of branches, knots, and seams and predictions of internal defect (e.g, Stängle et al. 2014). Also, since this method could retain the detailed shape of a stem, it is also possible to perform some product optimization algorithm, for example, fitting dimensional lumber to the stem to minimize waste. Notably, volume estimates from the unwrapping method, when compared to volume estimates from stem measurements combined with standard volume formulae, show biases that are consistent with previous studies comparing water displacement method and the same formulae (Martin 1984; Biging 1988; Filho et al. 2000). These biases likely represent failures of the formulae to capture actual detail in stem shape that is straightforward with an adequate point cloud.

A fundamental advantage of the unwrapping method is that it captures detail of the stem surface that is lost under contemporary alternatives. We consider the cylinder fitting method an extension of the traditional methods, where a section of a stem is considered as some type of primal geometry, into the digital world. However, the primal geometry used for cylinder fitting is cylinders instead of frustums of paraboloid or neiloid for traditional volume equations. This method along with the stem segmentation method developed by Raumonen et al. (2013) may yield an accurate estimate of tree volume, as well as a basic representation of the structure of the tree. However, this method does not catch details from the surface of the tree very well. For example, applying the QSM algorithm in 3DForest (https://www.3dforest.eu/) developed by Trochta et al. (2017) to our data reveals the algorithm to have some difficulties recording the large bump on Maple 1 (Fig. 6). Voxels can be considered a pixel in three dimension and can be used to preserve very good surface details, as well as provide an accurate volume estimation (Moskal and Zheng 2012; Hauglin et al. 2013; Hosoi et al.

Fig. 4. Clipped point cloud after registration (*a*), separated stem points (*b*), foliage points (*c*), and the resulting points for the 4.88 m log (*d*).

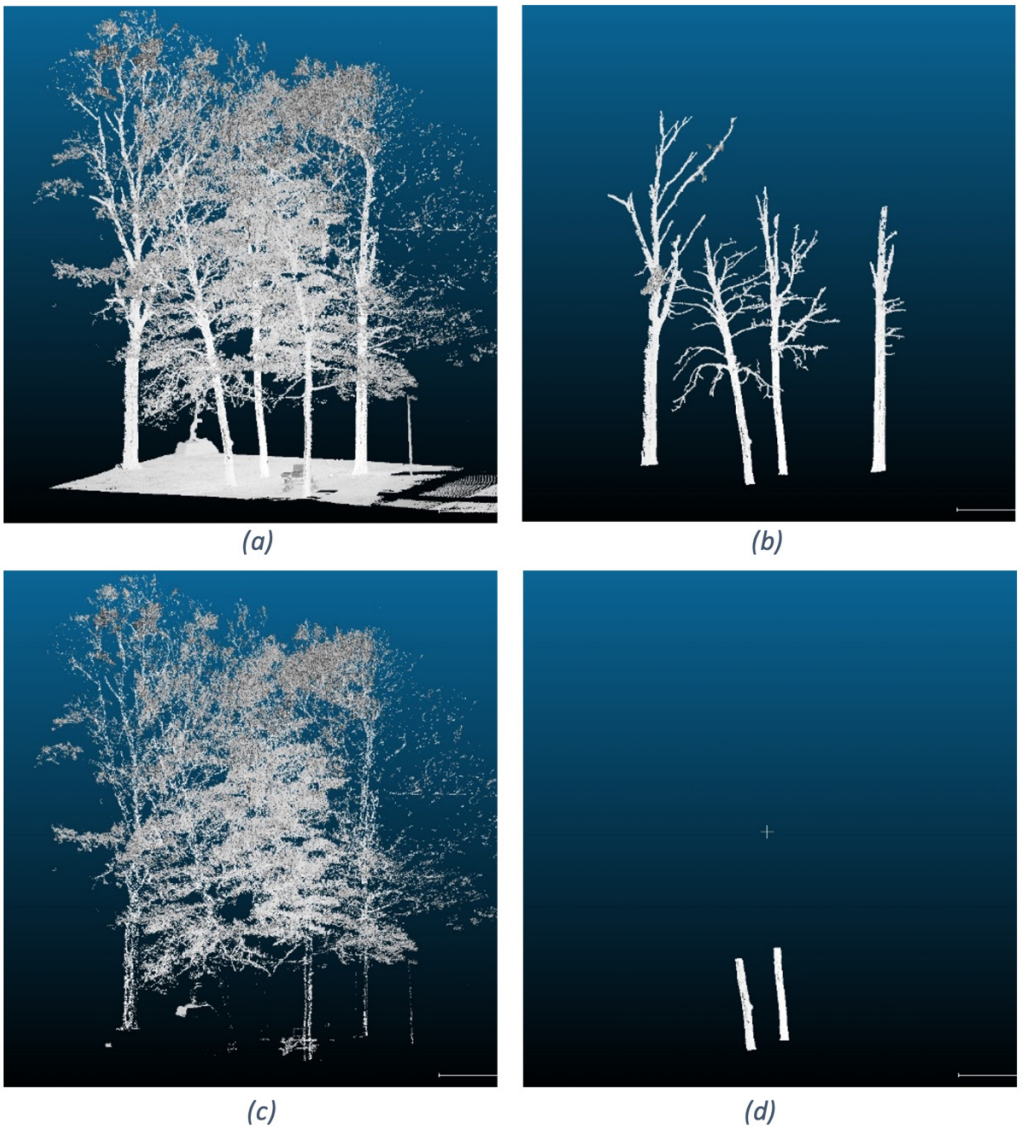

2013; Bienert et al. 2014). The unwrapping method shares some similar concepts with voxelization and the accuracies and details retained by both methods depend on the resolution (voxel size for voxelization and pixel size for unwrapping), but the unwrapping method does not require a fill algorithm to fill the inside of the tree. The outputs of the unwrapping method are simply 2D rasters and can be viewed without any special tools.

Incomplete information, either due to occlusion (e.g., brush, branches, or foliage) or insufficient scan points, is an issue that is common to methods that depend on point clouds. During field data collection, occlusion happens often, but can be minimized with good field methods. When dealing with an incomplete scan of a tree, methods that adopt a geometric primitive (e.g., an ellipse for diameter or a cylinder for volume) may be somewhat robust, since as long as the required parameter can be measured from the point cloud, a volume estimate can be generated. The voxelization method could use some sort of interpolation, such as spline interpolation (Hosoi et al. 2013), to counter the missing information, and a similar solution could be used for the unwrapping method. For small areas, this could be achieved within the workflow using IDW, but it would not work well if a large patch of a stem is missing. Because accuracy will decline under all approaches with missing information, we suggest that it is more important to acquire more complete data than to use algorithms to extrapolate over incomplete data. In practice, the use of handheld LiDAR systems that rely on Simultaneous Localization and Mapping (SLAM) algorithms for point cloud registration may have advantages compared to stationary units despite accuracy limitations, and this is an area of active contemporary research (e.g., Holopainen et al. 2013; Gollob et al. 2020; Hyyppä et al. 2020; Mokroš et al. 2021).

The apparent accuracy of the unwrapping method, when compared to volume estimated using Huber's, Newton's, and

Fig. 5. The unwrapped displacement (*a*), hillshade generated from the displacement raster (*b*), and the visualization of the stem section using a subdivided cylinder and the displacement raster in Blender (*c*).

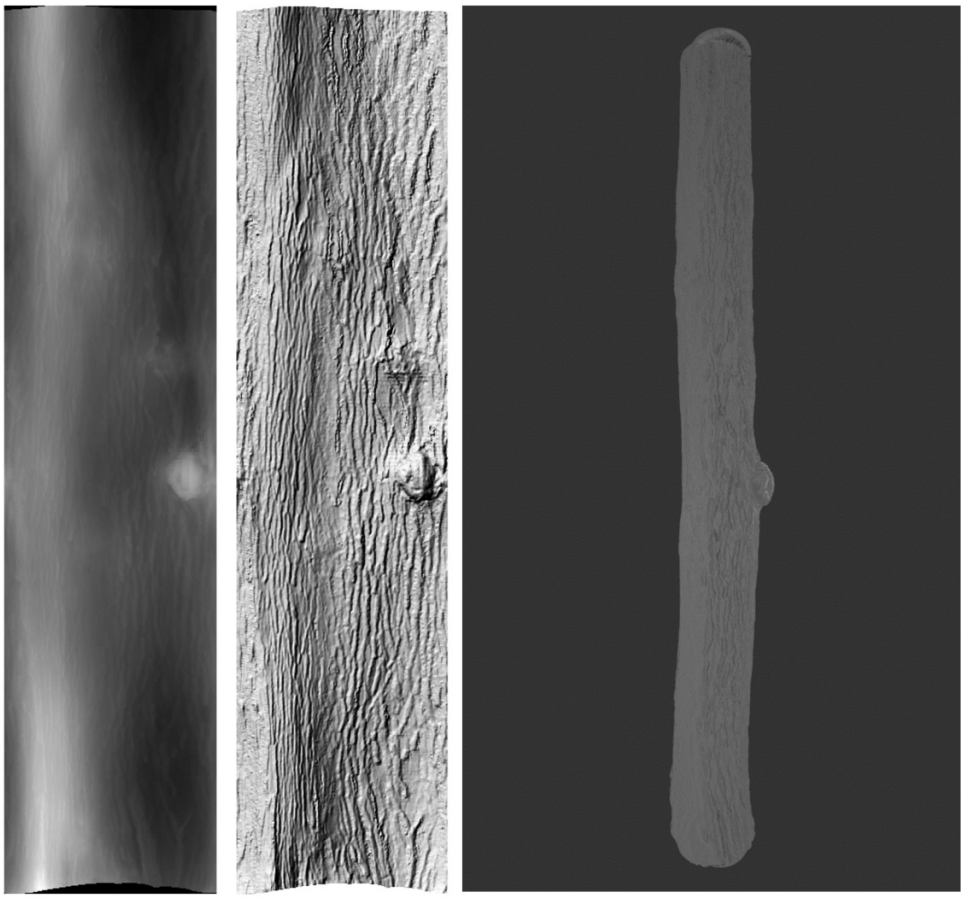

Smalians' formulas, and diameter measurements, is very similar to studies that make the same comparison using water displacement. Martin (1984) found the least bias for Huber's formula, followed by Newton's and then Smalian's, while Biging (1988) found for white pine log volume an error of less than 5% for 4.9 m logs for all formulae. Filho et al. (2000) found that for merchantable log volumes Huber's formula yield the least error, ranging from 2.99% to 6.35%, followed by Newton's formula, ranging from 3.33% to 11.39%, and Smalian's formula, ranging from 3.59% to 25.12%. In the present study, if the TLS-derived volume estimates are considered as the "true value," estimates using Huber's formula performed the best with a mean absolute bias of 5.51% for NC and 5.79% for CY, followed by Newton's formula with bias of 8.31% and 8.59% respectively, and Smalian's formula with bias of 9.71% and 10.00%, respectively. This seems consistent with the results from prior studies. While direct comparisons between LiDAR and water-displacement methods are ideal for accuracy assessment, the difficulties of performing such comparisons led to the use of simulated objects instead of field measurements. For example, Åkerblom et al. (2015) used only simulated shapes in an extensive examination of the effects of different primary geometries on volume estimation. In our study, we use field measurements that capture the actual taper profile of the stem as the reference, providing a more practical comparison. The similarities between our results and prior studies that use water displacement lends strength to the inference that the unwrapping method when compared to the formulae, can be closer to water displacement.

Systematic differences between estimates from formulae and the unwrapping method could be the result of one or more of the following reasons: (1) stem taper, (2) measurement error, (3) texture of the tree bark, and (4) artifacts on both ends of a log.

Stem taper

Smalian's, Huber's, and Newton's formulae eventually provide estimates of stem volume and represent different primitive shapes. Huber's and Smalian's formulae are for paraboloid frustum while Newton's formula is for neiloid frustum, and often Smalian's will overestimate and Huber's will underestimate if Newton's estimate is considered true (Kershaw et al. 2016). However, stem taper does not strictly follow a geometric shape, which is probably the major source of error. In this case, since the LiDAR estimates are considered more accurate, it makes sense that the biases used in this

Fig. 6. Illustration of QSM cylinder-fitting result (left) compared to the original point cloud (right). Note the irregularity imposed by the QSM algorithm (circled area). Illustrations generated in 3D Forest.

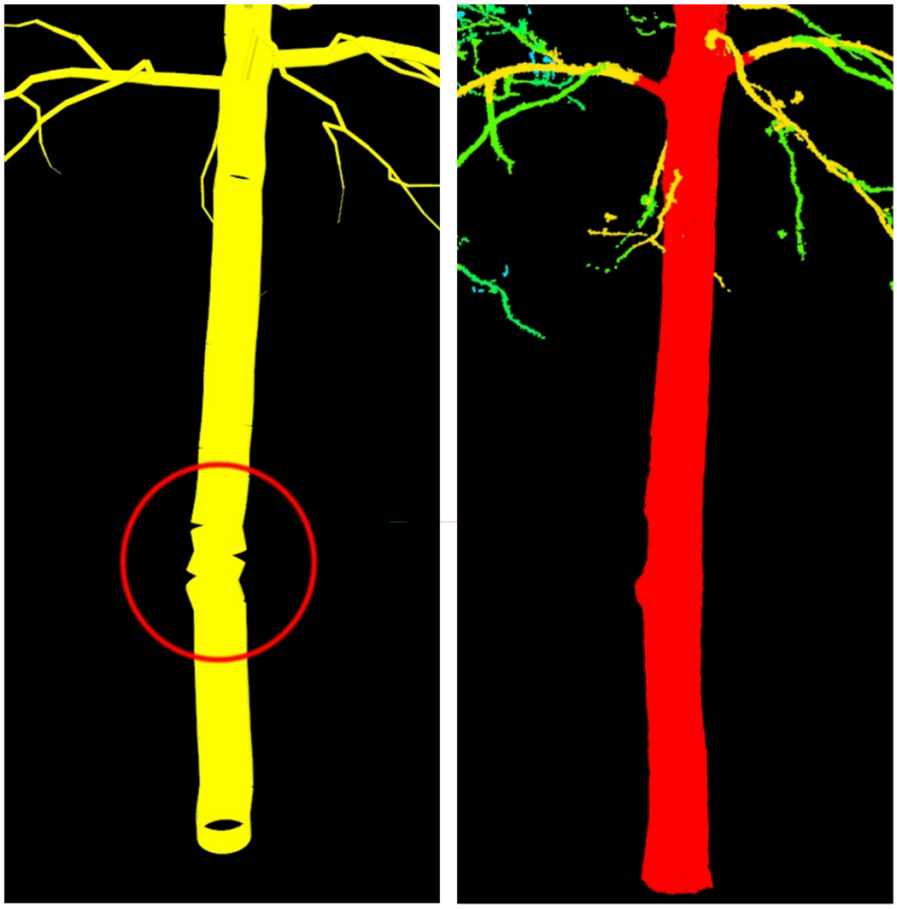

study are similar to studies comparing water displacement volume and the estimates from the formulae.

Measurement error

When taking diameter measurements using diameter tapes, accuracy is dependent on the tape being placed perpendicular to the central axis, and the tape being held snugly against the bole. Since this could be hard to achieve in practice, the measurements tend to overestimate the diameters of the bole (Avery and Burkhart 2002). Measurements using TLS point clouds have decreased point spacing and increased error with increasing distance from the scanner. For the upper stem, movements caused by wind are also more obvious than lower stem, which introduces larger error. At the same time, branches and foliage are more likely to cause occlusion leading to incomplete scan.

Bark texture and geometrical irregularities

Among all three species, the maples performed the worst compared to red pines and aspens (Table 1). Bark on the maples is observed to have coarser texture and the "cracks" are relatively deeper than the other two species, as is shown in Fig. 7. Also, when measuring the diameters using the diameter tape, the texture of the tree barks, even some depressions along the stem would be ignored, where it is like a convex hull applied to the cross section of the stem. Among the scanned trees, Maple 3 has a large cavity at the bottom of the stem and thus there are some overlapping points in the unwrapped points, as is shown in Fig. 8, and they cause some artifacts that could affect the volume estimation of the stem as well. Currently this method does not do well with such defects of a stem but could be solved by removing the overlapping points before unwrapping, which could introduce some error in the volume estimation. Due to geometrical irregularities, volume estimates obtained from primal geometries may also lead to overestimates. Witzmann et al. (2022) showed that estimates from primal geometry fitting to stem sections (using circles or ellipses) overestimated the cross-sectional areas. Algorithms such as cylinder fitting extend cross sections to three dimensions, and thus may also overestimate stem volume and the overestimation could be amplified by stem taper.

Artifacts on both ends of a log

The log point clouds were extracted by selecting the points between the ground and 4.88 m (16 ft) in height, but the stems all have slight lean. Thus, once the point cloud is rotated to follow the central axis, the top end is no longer a flat cut and the bottom end is usually slanted because of the terrain. One way to address this concern may be to use a spher-

Fig. 7. Example bark texture of maple (*a*), red pine (*b*), and aspen trees (*c*).

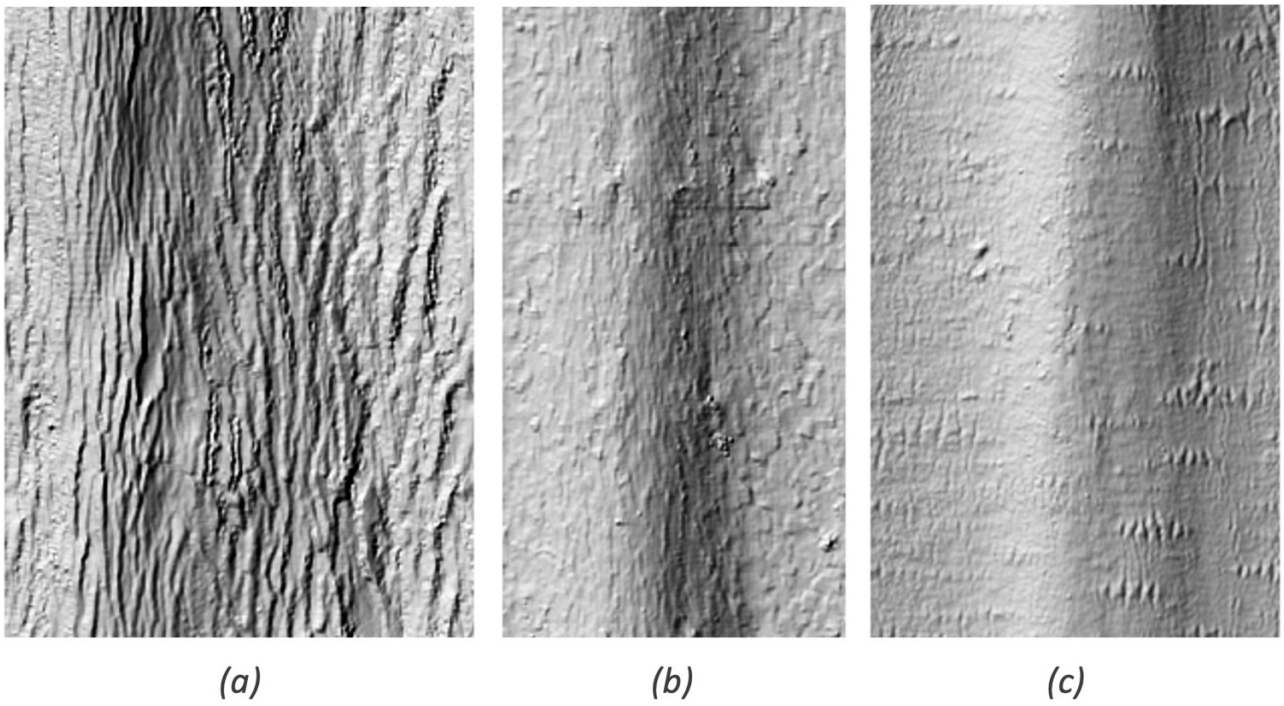

Fig. 8. The displacement raster (*a*) and the generated hillshade raster (*b*) of Maple 3. Note the artifacts caused by overlapping points from the large cavity (circled areas).

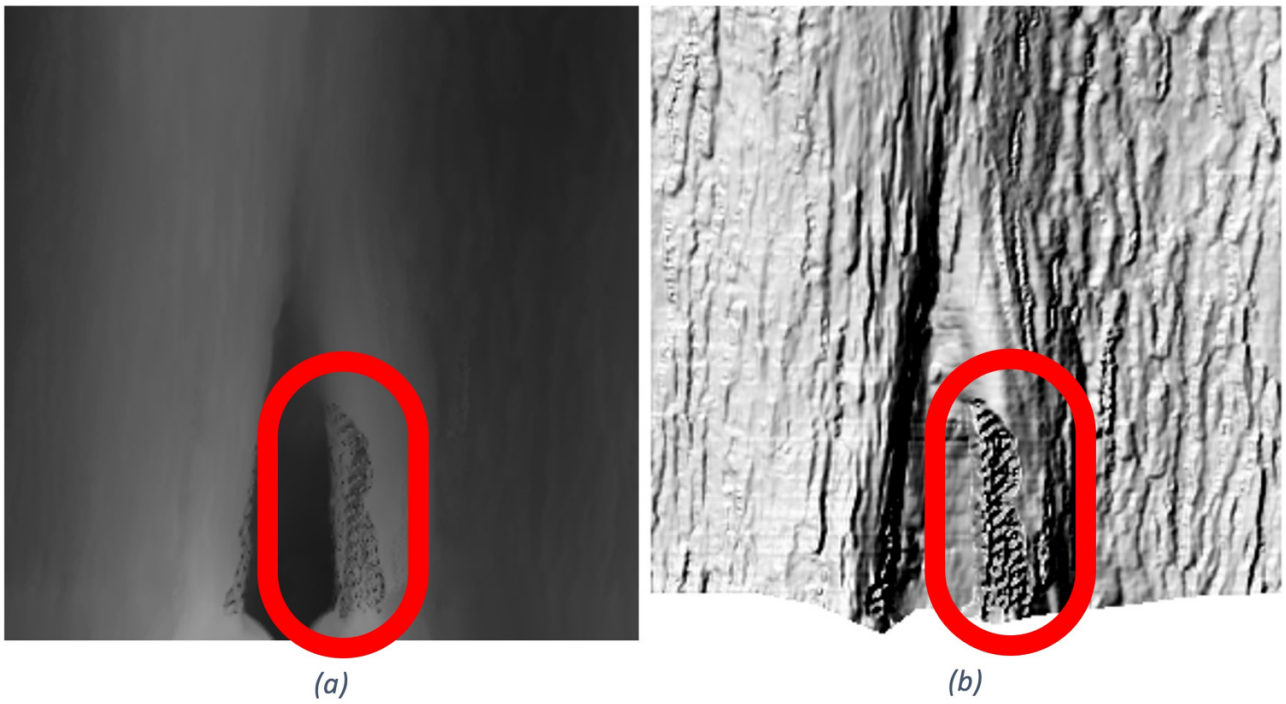

ical selection method, where the center of a sphere is placed at the bottom and a 4.88 m radius is used to ensure a flat top.

The focus in this study was the lowest 4.88 m (16 ft) log of standing trees and the sampled trees are straight enough to allow a straight line, which is the central axis, to be contained within the log (Fig. 9*a*). However, if the length of the log is extended, it is likely to eventually encounter a bend significant enough that the central axis is no longer contained, inducing error of the volume estimate (Fig. 9*b*). Other than excessive bend in a single stem, the major branches or fork in the upper stem of some trees will have the same behavior and thus some sort of segmentation of the stem will be

Fig. 9. Illustrations of a stem straight enough to allow a line pass through (*a*) and a crooked stem where there will be overlapping points once unwrapped (*b*).

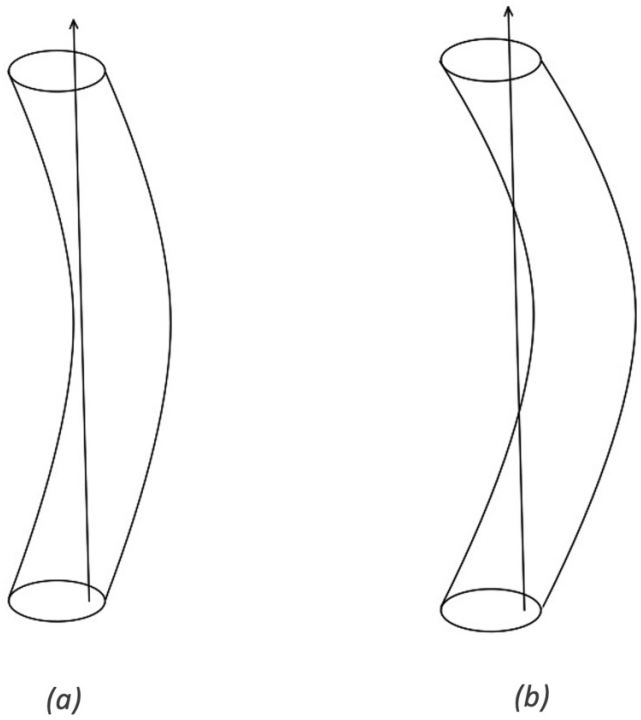

required. Segmentation and reconstruction algorithms from QSM (Raumonen et al. 2011; Åkerblom et al. 2012; Raumonen et al. 2013) could be potentially used in combination with the unwrapping method. In QSM, segments are defined by bifurcation (i.e., branches), and are divided into smaller successive pieces termed "regions," each of which is then approximated with cylinders. Raumonen et al. (2013) note that long regions are preferred in QSM because they are more robust to noise, outliers, and imperfect point clouds, but may need to be subdivided into many shorter regions to better follow the radius and direction of the segment. Since the unwrapping method is limited only by the need to contain the central axis, it may confer benefits in the context of QSM because the need to subdivide into short regions is avoided.

Conclusion

In this study, we proposed and developed a method of estimating tree stem volume, combining concepts of cylinder fitting, voxelization, and DEM volume estimation. The method is consistent with prior studies where volume estimation from often used equations is compared to water-displaced volume. This method will not only generate an accurate estimate of a tree stem, but also generate a 2D raster similar to a DEM that can be easily visualized. From the 2D rasters, we were also able to identify some major defects from the surface of the stems, as well as small details. In future work, we aim to integrate tree segmentation to this method, which could also provide volume estimation for the upper stem structures.

Acknowledgements

We thank James M. Schmierer for help during the data collection and Ann Maclean for providing expertise in ArcGIS. We also appreciate the suggestions from two anonymous reviewers and the associate editor, which helped improve the manuscript.

Article information

History dates
Received: 1 June 2022
Accepted: 7 October 2022
Accepted manuscript online: 11 October 2022
Version of record online: 15 December 2022

Data availability
Data are available from the authors upon reasonable request.

Author information

Author ORCIDs
Zhongming An https://orcid.org/0000-0001-9918-1734
Robert E. Froese https://orcid.org/0000-0003-0627-3088

Author notes
Robert E. Froese served as an Associate Editor at the time of manuscript review and acceptance; peer review and editorial decisions regarding this manuscript were handled by Jari Vauhkonen.

Author contributions
REF conceived the presented idea and acquired funding. ZA developed the methodology, collected and curated data, and completed formal analysis. ZA and REF prepared visualizations, ZA wrote the original draft, and ZA and REF completed review and editing.

Competing interests
The authors have no relevant financial or non-financial interests to disclose

Funding information
Partial funding for this work was provided by the Ecosystem Science Center at Michigan Technological University.

References

Åkerblom, M., Raumonen, P., Kaasalainen, M., Kaasalainen, S., and Kaartinen, H. 2012. Comprehensive quantitative tree models from TLS data. *In* Proceedings of 2012 IEEE International Geoscience and Remote Sensing Symposium (IGARSS), Munich, Germany, 22–27 July 2012. pp. 6507–6510.

Åkerblom, M., Raumonen, P., Kaasalainen, M., and Casella, E. 2015. Analysis of geometric primitives in quantitative structure models of tree stems. Remote Sens. **7**: 4581–4603.

Avery, T.E., and Burkhart, H.E. 2002. Forest measurements. 5th ed. McGraw-Hill, Boston, MA, USA.

Biging, G.S. 1988. Estimating the accuracy of volume equations using taper equations of stem profile. Can. J. For. Res. **18**: 1002–1007. doi:10.1139/x88-153.

Bienert, A., Hess, C., Maas, H.G., and von Oheimb, G. 2014. A voxel-based technique to estimate the volume of trees from terrestrial laser scanner data. Int. Arch. Photogramm. Remote Sens. Spat. Inf. Sci.—ISPRS Arch. **40**(5): 101. doi:10.5194/isprsarchives-XL-5-101-2014.

Calders, K., Newnham, G., Burt, A., Murphy, S., Raumonen, P. Herold, M., et al. 2014. Nondestructive estimates of above-ground biomass using terrestrial laser scanning. Methods Ecol. Evol. **6**: 198–208. doi:10.1111/2041-210X.12301.

Calders, K., Origo, N., Burt, A., Disney, M., Nightingale, J., Raumonen, P., et al. 2018. Realistic forest stand reconstruction from terrestrial LiDAR for radiative transfer modelling. Remote Sens. **10**: 933: 1–15. doi:10.3390/rs10060933.

Filho, A.F., Machado, S.A., and Carneiro, M.R.A. 2000. Testing accuracy of log volume calculation procedures against water displacement techniques (xylometer). Can. J. For. Res. **30**: 990–997. doi:10.1139/x00-006.

Gollob, C., Ritter, T., and Nothdurft, A. 2020. Forest inventory with long range and high-speed personal laser scanning (PLS) and simultaneous localization and mapping (SLAM) technology. Remote Sens. **12**(9): 1509. doi:10.3390/rs12091509.

Grohmann, C.H., Garcia, G.P.B., Affonso, A.A., and Albuquerque, R.W. 2020. Dune migration and volume change from airborne LiDAR, terrestrial LiDAR and structure from motion-multi view stereo. Comput. Geosci. **143**: 104569. doi:10.1016/j.cageo.2020.104569.

Hackenberg, J., Spiecker, H., Calders, K., Disney, M., and Raumonen, P. 2015. SimpleTree—an efficient open source tool to build tree models from TLS clouds. Forests, **6**: 4245–4294. doi:10.3390/f6114245.

Hauglin, M., Astrup, R., Gobakken, T., and Næsset, E. 2013. Estimating single-tree branch biomass of Norway spruce with terrestrial laser scanning using voxel-based and crown dimension features. Scand. J. For. Res. **28**(5): 456–469. doi:10.1080/02827581.2013.777772.

Holopainen, M., Kankare, V., Vastaranta, M., Liang, X., Lin, Y., Vaaja, M., et al. 2013. Tree mapping using airborne, terrestrial and mobile laser scanning–A case study in a heterogeneous urban forest. Urban For. Urban Green. **12**(4): 546–553.

Hosoi, F., Nakai, Y., and Omasa, K. 2013. 3-D voxel-based solid modeling of a broad-leaved tree for accurate volume estimation using portable scanning lidar. ISPRS J. Photogramm. Remote Sens. **82**: 41–48. doi:10.1016/j.isprsjprs.2013.04.011.

Hyyppä, E., Yu, X., Kaartinen, H., Hakala, T., Kukko, A., Vastaranta, M., and Hyyppä, J. 2020. Comparison of backpack, handheld, under-canopy UAV, and above-canopy UAV laser scanning for field reference data collection in boreal forests. Remote Sens. **12**(20): 3327. doi:10.3390/rs12203327.

Kershaw, J.A., Jr, Ducey, M.J., Beers, T.W., and Husch, B. 2016. Forest mensuration. John Wiley & Sons.

Liu, X. 2008. Airborne LiDAR for DEM generation: some critical issues. Prog. Phys. Geogr. **32**(1): 31–49.

Ma, R. 2005. DEM generation and building detection from LiDAR data. Photogramm. Eng. Remote Sens. **71**(07): 847–854. doi:10.14358/PERS.71.7.847.

Martin, A.J. 1984. Testing volume equation accuracy with water displacement techniques. For. Sci. **30**(1): 41–50.

McNabb, R., Nuth, C., Kääb, A., and Girod, L. 2019. Sensitivity of glacier volume change estimation to DEM void interpolation. The Cryosphere, **13**(3): 895–910. doi:10.5194/tc-13-895-2019.

Mokroš, M., Mikita, T., Singh, A., Tomaštík, J., Chudá, J., Wężyk, P., et al. 2021. Novel low-cost mobile mapping systems for forest inventories as terrestrial laser scanning alternatives. Int. J. Appl. Earth Obs. Geoinf. **104**: 102512. doi:10.1016/j.jag.2021.102512.

Moskal, L.M., and Zheng, G. 2012. Retrieving forest inventory variable with terrestrial laser scanning (TLS) in urban heterogeneous forest. Remote Sens. **4**: 1–20. doi:10.3390/rs4010001.

Olschofsky, K., Mues, V., and Köhl, M. 2016. Operational assessment of aboveground tree volume and biomass by terrestrial laser scanning. Comput. Electron. Agric. **127**: 699–707. doi:10.1016/j.compag.2016.07.030.

Parker, R.C. 1997. Nondestructive sampling applications of the telerelaskop in forest inventory. South. J. Appl. For. **21**(2): 75–83. doi:10.1093/sjaf/21.2.75.

Raumonen, P., Kaasalainen, S., Kaasalainen, M., and Kaartinen, H. 2011. Approximation of volume and branch size distribution of trees from laser scanner data. Int. Arch. Photogramm. Remote Sens. Spat. Inf. Sci. **38**(5/W12): 79–84.

Raumonen, P., Kaasalainen, M., Åkerblom, M., Kaasalainen, S., Kaartinen, H., Vastaranta, M., et al. 2013. Fast automatic precision tree models from terrestrial laser scanner data. Remote Sens. **5**: 491–520. doi:10.3390/rs5020491.

Shan, J., and Sampath, A. 2005. Urban DEM generation from raw LiDAR data: a labeling algorithm and its performance. Photogramm. Eng. Remote Sens. **71**(02): 217–226. doi:10.14358/PERS.71.2.217.

Stängle, S.M., Brüchert, F., Kretschmer, U., Spiecker, H., and Sauter, U.H. 2014. Clear wood content in standing trees predicted from branch scar measurements with terrestrial LiDAR and verified with X-ray computed tomography. Can. J. For. Res. **44**(2): 145–153. doi:10.1139/cjfr-2013-0170.

Stovall, A.E.L., Anderson-Teixeira, K.J., and Shugart, H.H. 2018. Assessing terrestrial laser scanning for developing non-destructive biomass allometry. For. Ecol. Manage. **427**: 217–229. doi:10.1016/j.foreco.2018.06.004.

Sun, Y., Liang, X., Liang, Z., Welham, C., and Li, W. 2016. Deriving merchantable volume in poplar through a localized tapering function from non-destructive terrestrial laser scanning. Forests, **7**: 87: 1–11. doi:10.3390/f7040087.

Thies, M., Pfeifer, N., Winterhalder, D., and Gorte, B.G.H. 2004. Three dimensional reconstruction of stems for assessment of taper, sweep and lean based on laser scanning of standing trees. Scand. J. For. Res. **19**(6): 571–581. doi:10.1080/02827580410019562.

Trochta, J., Krůček, M., Vrška, T., and Král, K. 2017. 3D Forest: an application for descriptions of three-dimensional forest structures using terrestrial LiDAR. PLoS ONE, **12**(5): e0176871. doi:10.1371/journal.pone.0176871. PMID: 28472167.

Witzmann, S., Matitz, L., Gollob, C., Ritter, T., Kraßnitzer, R., Tockner, A., et al. 2022. Accuracy and precision of stem cross-section modeling in 3D point clouds from TLS and caliper measurements for basal area estimation. Remote Sens. **14**(8): 1923. doi:10.3390/rs14081923.

You, L., Wei, J., Liang, X., Lou, M., Pang, Y., and Song, X. 2021. Comparison of numerical calculation methods for stem diameter retrieval using terrestrial laser data. Remote Sens. **13**(9): 1780. doi:10.3390/rs13091780.

Zhang, W., Qi, J., Wan, P., Wang, H., Xie, D., Wang, X., and Yan, G. 2016. An easy-to-use airborne LiDAR data filtering method based on cloth simulation. Remote Sens. **8**(6): 501. doi:10.3390/rs8060501.

Zhang, W., Wan, P., Wang, T., Cai, S., Chen, Y., Jin, X., and Yan, G. 2019. A novel approach for the detection of standing tree stems from plot-level terrestrial laser scanning data. Remote Sens. **11**(2): 211. doi:10.3390/rs11020211.